Research Journal of Applied Sciences, Engineering and Technology 4(9): 1172-1180, 2012
ISSN: 2040-7467
© Maxwell Scientific Organization, 2012
Submitted: January 10, 2012 Accepted: January 29, 2012 Published: May 01, 2012

Strengthening of RC Beams with Large Openings in Shear by CFRP Laminates: Experiment and 2D Nonlinear Finite Element Analysis

S.C. Chin, N. Shafiq and M.F. Nuruddin
Civil Engineering Department, Universiti Teknologi PETRONAS, Malaysia

Abstract: This study presents the experimental study and numerical analysis of Reinforced Concrete (RC) beams with large square openings placed in the shear region, at a distance 0.5d and d away from the support, strengthened by Carbon Fiber Reinforced Polymer (CFRP) laminates. This research aims to investigate the strength losses in RC beam due to the presence of large square openings placed at two different locations in shear region. Also, in order to re-gain the beam structural capacity loss due to the openings, strengthening by CFRP laminates around the openings were studied. A total of six RC beams were tested to failure under four point loading including control beams, un-strengthened and strengthened RC beams with large square openings in shear region at a distance 0.5d and d away from the support. The CFRP strengthening configuration considered in this study was a full wrapping system around the square openings. A nonlinear finite element program, ATENA was used to validate the results of the tested beams. Comparisons between the finite element predictions and experimental results in terms of crack patterns and load deflection relationships are presented. The crack pattern results of the finite element model show good agreement with the experimental data. The load midspan deflection curves of the finite element models exhibited a stiffer result compared to the experimental beams. The possible reason may be due to the perfect bond assumption between the concrete and steel reinforcement.

Key words: CFRP, large opening, RC beam, square, strengthening

INTRODUCTION

Generally, holes or openings are usually found in floors due to staircase, elevators, ducts and pipes. Openings are provided through the floor beams to facilitate the passage of utility pipes and service ducts. These service ducts accommodate essential services such as conduits, power supply, water and drainage pipes, ventilation system, air-conditioning and network system access or even for inspection purposes in beam structures. These arrangements of building services resulted in a significant reduction in headroom, minimize the storey height and results in major savings in material and construction cost especially in multi-storey buildings and tall building construction (Mansur and Tan, 1999). However, the presence of opening in the web of a reinforced concrete beam resulted to many problems in the beam behaviour including reduction in beam stiffness, excessive cracking and deflection and reduction in beam capacity. Furthermore, inclusion of openings leads to high stress concentration around the openings especially at the opening corners. The reduction of area in the total cross sectional dimension of a beam changes the simple beam behaviour to a more complex one (Mansur *et al*., 1992; Mansur, 2006).

If openings are to be provided in existing beams especially in the shear zone, sufficient treatment and attention is needed to ensure the safety and serviceability of the structure. In general, shear failure of concrete structures is catastrophic due to the brittle nature and the fact of no advance warning prior to failure. Thus, in an existing beam, strengthening externally around the opening is crucial with the use of external reinforcing material, such as steel plates or by Fiber Reinforced Polymer (FRP) materials.

The application of FRP as external reinforcement to strengthen RC beams has received much interest from the research community. The most common type of FRP in the concrete industry is made with carbon, aramid or glass fibers. The FRPs are usually in the form of sheets, strips, wraps or laminates. These materials were applied by bonding it to the external surfaces of the beams with various configurations and layouts. The usage of FRPs to repair and rehabilitate damaged steel and concrete structures has become increasingly attractive as the FRPs are well-known with good mechanical properties, particularly with its high strength to weight ratio and low weight.

To date, the literatures available for the study of RC beams with openings strengthened by CFRP laminates are

Corresponding Author: S.C. Chin, Civil Engineering Department, Universiti Teknologi PETRONAS, Malaysia

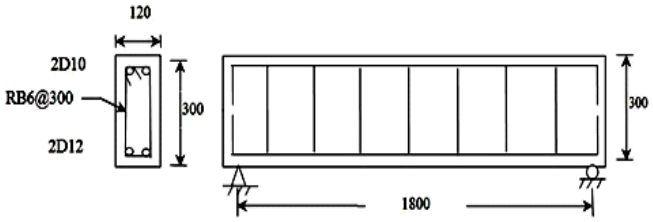

Fig. 1: Beam reinforcement details (Unit: mm)

rather limited. Mansur *et al*. (1999) investigated the use of FRP plates for strengthening reinforced concrete T-beams with small circular opening. Abdalla *et al*. (2003) and Allam (2005) studied the shear strengthening of reinforced concrete beams with rectangular opening using FRP sheets. Meanwhile, El Maaddawy and Sherif (2009) investigated the use of FRP sheets for shear strengthening of reinforced concrete deep beams with square openings.

As far as numerical modelling is concerned, the numerical investigations of RC beam with openings are somewhat limited, particularly with the use of finite element method. Madkour (2009) proposed a theoretical approach to analyze the efficiency of applying CFRP laminates as an external strengthening technique in a three dimensional domain to determine the effective and economic strengthening configuration. On the other hand, an experimental program was supplemented by a nonlinear finite element analysis by Pimanmas (2010) to simulate the behaviour of specimens in the experiment. The research studied the strengthening of reinforced concrete beams with circular and square opening by externally installed FRP rods.

In this study, the experimental results of six reinforced concrete beams are presented. The experimental program addresses the behaviour of RC beams with the presence of large square openings in shear region; at a distance 0.5d and d away from the support, the loss of structural capacity due to large square openings, and the efficiency of using a full wrapping system of CFRP laminates around the openings at a distance 0.5d and d away from the support. The results in terms of crack pattern, failure mode, ultimate load and load versus deflection relationship are presented. For validation, a non-linear finite element program, ATENA is used to simulate the tested beams. Comparisons of the predicted results with the experimental data are presented.

MATERIALS AND METHODS

The investigation conducted in this study covers the experimental testing and numerical analysis using a non-linear finite element program. The materials and methodology are presented as follows:

Experimental program: In the experimental program, a total of six RC beams were tested to failure under four point loading to investigate the structural behaviour including crack patterns, failure mode, ultimate load and load-deflection relationship. The opening region was strengthened by CFRP laminates to re-gain the loss of structural capacity.

Material characteristics: The concrete used in the experimental study was ready-mixed concrete designed for 28 days compressive strength of 35 MPa. The water cement ratio was 0.54. The coarse aggregate was 20 mm granite crushed aggregate. Fine sand as fine aggregate was used. The longitudinal steel reinforcement was deformed steel bars with nominal yield strength of 410 MPa. The web reinforcement was mild steel with nominal yield strength of 275 MPa. The CFRP laminates were unidirectional with a width of 100 mm and a thickness of 1.4 mm. The modulus of elasticity, E of CFRP laminates was 170 GPa. CFRP laminates were applied after the beams were cast. To ensure a suitable surface preparation for bonding, the beam surface were brushed and cleaned before the application of CFRP laminates. The laminates were bonded to the specimens with an epoxy resin, Sikadur 30. The thickness of a cured CFRP laminates bonded to the specimen is typically 3 mm.

Test specimen: A schematic diagram of the test specimen showing the reinforcement details is depicted in Fig. 1. The test specimen was 2000 mm long with a rectangular cross section of 120×300 mm. The effective depth to the main reinforcement was 280 mm while the effective span of the beam was 1800 mm. The tension steel reinforcement consisted of two diameter 12 mm deformed steel bars each having a nominal cross section area of A = 113 mm^2. The compression steel reinforcement consisted of two diameter 10 mm deformed steel bars with A = 79 mm^2 for each bars. The stirrups consisted of diameter 6 mm smooth bars with A = 28 mm^2 each spaced at 300 mm center to center.

In this study, large square opening was considered. The size of the square opening was 210×210 mm. The ratio of the opening size to the beam's effective depth was

Table 1: Beam specimens

Bean	Shape	Location	Condition
B1	Control	NA	-
B2	Control	NA	-
B3	Square	0.5d	Without Strengthening
B4	Square	d	Without Strengthening
B5	Square	0.5d	Strengthening
B6	Square	d	Strengthening

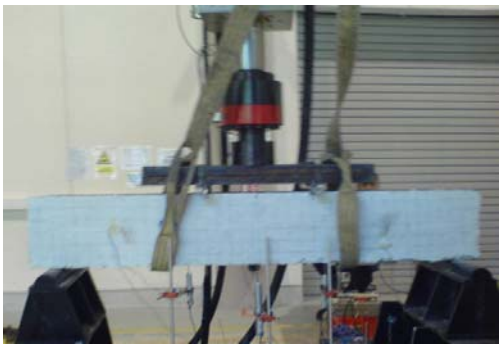

Fig. 2: Test setup

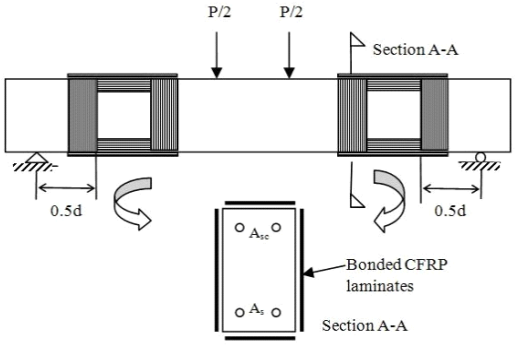

Fig. 3: CFRP strengthening configuration

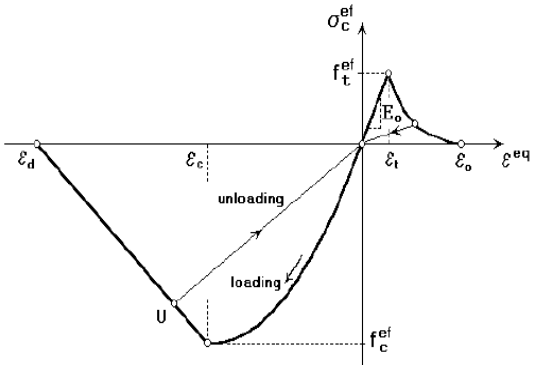

Fig. 4: Uniaxial stress strain law for concrete

0.75 in which researchers may consider it as large opening (Mansur, 2006; Pimanmas, 2010). The beams were cast in a horizontal position using plywood formwork. The large square opening was formed by inserting a box fabricated from plywood placed at both shear zone of the beam.

The beam specimens are listed in Table 1. A total of six RC beams were cast. The beams consisted of two solid control beams without opening, two beams without strengthening with large square openings at 0.5d and d away from the support and remaining two beams with large square openings at distance 0.5d and d away from the support for strengthening by CFRP laminates.

Test setup: The beam specimens were tested until failure under four point loading with static load using a Universal Testing Machine (UTM) of 500 kN. The test setup is shown in Fig. 2. A spreader beam was used to transfer the load to the test specimen through two loading points at 500 mm apart. The beam deflection was monitored by a number of linear variable displacement transducers (LVDTs) placed at the bottom soffit of the beam. The crack development and propagation were marked and the mode of failure was recorded.

CFRP strengthening configuration: Figure 3 shows the strengthening configuration of CFRP laminates in beam with large square openings placed at a distance 0.5d away from the support, beam B5. The large square openings in the shear region were fully wrapped by CFRP laminates; at both surfaces around the openings, at tension and compression zone. The length of CFRP laminates used in this study was 410, 300 and 210 mm. The CFRP laminates were 1.4 mm thick with 100 and 45 mm width. To investigate the effectiveness of the strengthening configuration with openings placed at different locations, similar strengthening configuration with CFRP laminates were applied onto beam with large square openings at distance d away from the support, beam B6.

2D non-linear finite element modelling: In this study, a two dimensional nonlinear finite element analysis was conducted using the finite element package, ATENA. The numerical predictions are compared to the test results.

Material models: For the concrete, the constitutive model of the finite element package ATENA (Cervenka *et al*., 2010) is used. In this approach, the elastic constants are derived from a stress-strain function known as equivalent uniaxial law which covers the complete range of the plane stress behaviour in tension and compression. For the stress-strain relationship of the concrete in compression, the formula recommended by CEB-FIP Model Code 90 has been adopted for the ascending branch. The elastic limit of the maximum concrete compressive strength is reached followed by a nonlinear behaviour until the maximum concrete strength is reached. The softening law in compression is linearly descending.

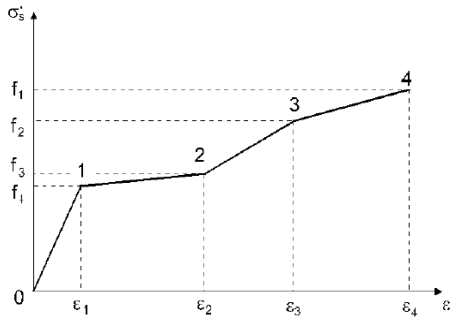

Fig. 5: Multi-linear stress strain law for reinforcement

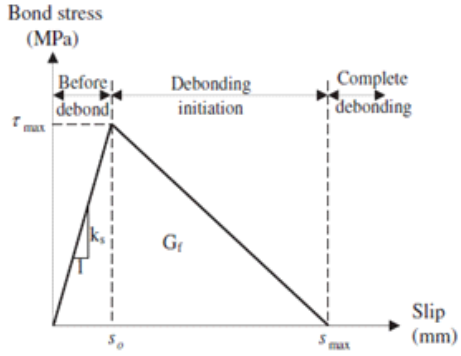

Fig. 6: Bond slip model

An ascending-descending behaviour for the concrete in tension is adopted. The slope of the ascending branch is equal to the concrete modulus of elasticity. In the descending branch of the stress-strain curve, a fictitious crack model based on a crack-opening law and fracture energy is used, where the cracks occur when the principal stress exceeds the tensile strength. In this study, rotated crack model in the smeared cracking approach is adopted. Poisson's ratio for concrete is assumed to be 0.2. Fig. 4 shows the uniaxial stress strain law for concrete.

The steel is represented by multi-linear law which consists of four lines as shown in Fig. 5. This law allows a linear modelling all four stages of steel behaviour: elastic state, yield plateau, hardening and fracture. The stress and strain of the steel reinforcement were measured in the experimental study. These values were used in the FEM model. A Poisson's ratio of 0.3 is used for steel reinforcement. The bond between steel reinforcement and concrete is assumed as a perfect bond. A linear elastic orthotropic constitutive relation is assumed for the FRP composites. A rupture point on the stress strain relationship for the fiber direction defines the ultimate stress and strain of the FRP.

FRP/concrete interface: A bond slip model developed by Lu *et al*. (2005) shown in Fig. 6 is adopted. This bond slip model is considered as an accurate bond slip model that can be incorporated into finite element analysis (Godat *et al*., 2007b; Kotynia *et al*., 2008; Obaidat *et al*., 2010; Godat *et al*., 2011). The mechanical behaviour of the FRP/concrete interface was modelled as a relationship between the local shear stress, τ and relative displacement, s between the CFRP laminate and the concrete. The τ –s relationship is given by (Kotynia *et al*., 2008):

$$\tau = \tau_{max}\sqrt{s / s_o} \quad if \quad s \le s_o \tag{1}$$

$$\tau = \tau_{max}\exp[-\alpha(s / s_o - 1)] \; if \quad s \ge s_o \tag{2}$$

The maximum bond strength τ_{max} and the corresponding slip s_o are governed by the tensile strength of the concrete f_t and a width ratio parameter β_w as follows:

$$\tau_{max} = 1.5\beta_w f_t \tag{3}$$

$$s_o = 0.0195\beta_w f_t \tag{4}$$

The parameter β_w is defined in terms of the CFRP laminate width b_f and the width of the beam b_c as follows:

$$\beta_w = \sqrt{\frac{2.25 - b_f / b_c}{1.25 + b_f / b_c}} \tag{5}$$

The area under the τ –s curve indicates the interfacial fracture energy G_f which corresponds to the energy per unit bond area required for complete debonding; which is calculated as follows:

$$G_f = 0.308\beta^2{}_w\sqrt{f_t} \tag{6}$$

The difference in relative displacement between the concrete and CFRP laminate represents the slip at the interface.

Geometrical modelling: To represent the concrete, SBETA material model for two dimensional plane stress elements was used. The tensile behaviour of concrete was modelled by a combination of nonlinear fracture mechanics with the crack band method, in which the smeared crack concept was adopted. The steel reinforcement, stirrups and CFRP laminates were modelled by a single straight line in a discrete manner by bar reinforcement elements. Full bond is assumed between the steel reinforcement and the surrounding concrete. The bond slip relation of CFRP and concrete was defined and assigned in the properties of discrete reinforcement bar of CFRP.

Nonlinear solution: In this investigation, a displacement-controlled incremental loading method was employed with an iterative solution procedure based on the Newton-Raphson method was adopted.

RESULTS AND DISCUSSION

Test results:

Crack pattern: The control beams without opening, B1 and B2 failed in shear mode as observed. In the experiment, crack lines appeared at the tension zone and penetrated vertically up to the neutral axis of the beam. It was observed that the flexural cracks increased in numbers followed by the formation of diagonal cracks. The crack width increased before failure, bringing an abrupt brittle failure at the shear zone. The shear failure were seen initiated at the point of the applied load to the support as the bottom reinforcements yielded; crushing of concrete cover was observed at the left point load and at the left support. Similar mode of failure was identified for both control beams, B1 and B2. Fig. 7a and b show the crack pattern and failure mode of both control beams, respectively.

Beam B3 represents a reinforced concrete beam with both large square openings placed in the shear region of the beam, at a distance 0.5d away from the support. Initially, a crack was observed at the top right corner and bottom left corner followed by the remaining corners of the square opening near the left support. Similarly, minor cracks were observed at the four corners of the square opening near the right support. However, the crack condition is not as severe as the left opening. The crack pattern and failure mode of beam B3 is illustrated in Fig. 7c. The beam failed in shear with diagonal cracks initiated from the right corner towards the point load while cracks at the bottom left corner were seen penetrated towards the edge of the beam. The large square opening on the left span was observed tilted slightly upwards while the opening position on the right remained undisturbed. Yielding of top steel reinforcement at the left square opening was noticed.

Fig. 7d shows the crack pattern and failure mode of beam B4. The beam B4 represents a reinforced concrete beam with large square openings located in shear region in the reinforced concrete beam, at a distance d away from the support. Similar to beam B3, minor cracks at the four corners of the square openings were observed in both openings. However, the cracks at the left square opening were clearly seen compared to the square opening on the right. A brittle shear failure was observed in beam B4. From Fig. 7d, it was found that the large square opening at a distance d from the left support tilted slightly upwards due to yielding of top and bottom steel reinforcements. Diagonal cracks from the corners of the square opening were seen penetrated to the left point load and to the left support. Crushing of concrete cover was seen at the bottom chord below the opening and the area near to the support. Likewise in beam B3, the shape of the square opening near the right support remains unchanged.

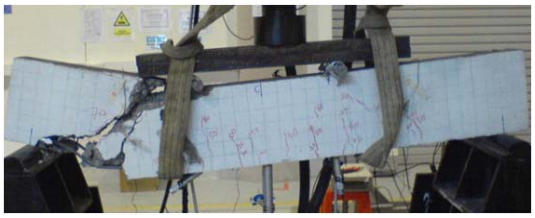

(a) B1

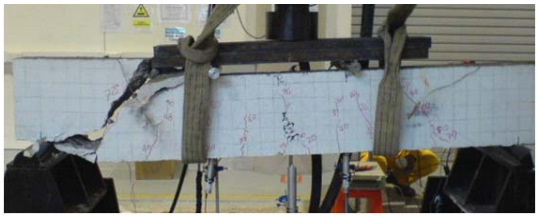

(b) B2

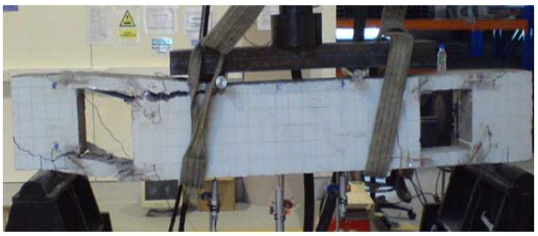

(c) B3

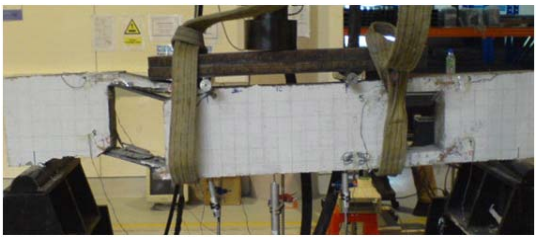

(d) B4

Fig. 7: Crack pattern and failure mode of control beams and un-strengthened beams

Beam B5 denotes the RC beam with large square openings strengthened by CFRP laminates at a distance 0.5d away from the support. Fig. 8a shows the crack pattern and failure mode of the beam. Flexural cracks were observed along the mid-span until an abrupt shear failure was occurred. The beam was failed in shear at the

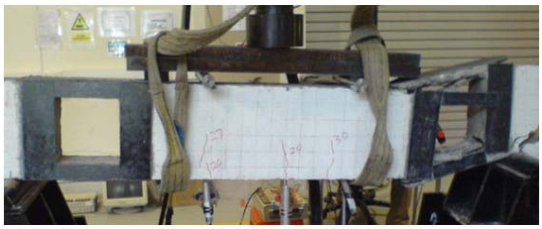

(a) B5

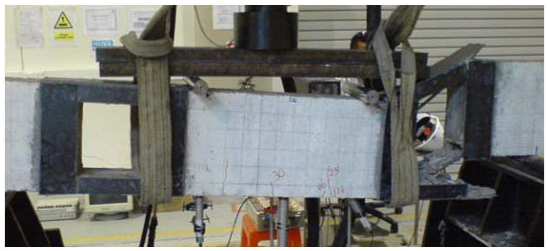

(b) B6

Fig. 8 : Crack pattern and failure mode of strengthened beams

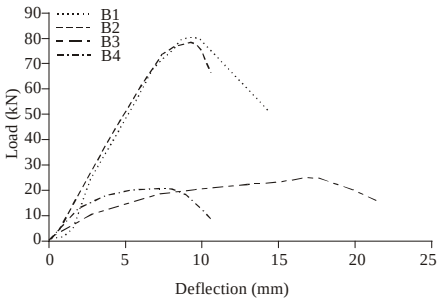

Fig. 9: Load deflection relationship of un-strengthened beams compared with control beams

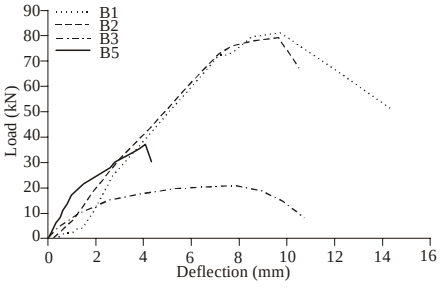

Fig. 10: Load deflection relationship of un-strengthened and strengthened beams with large square openings at distance 0.5d

square opening near the right support, a different failure direction was observed compared to un-strengthened beam, B3. The square opening was tilted upwards due to yielding of top and bottom steel reinforcement causing

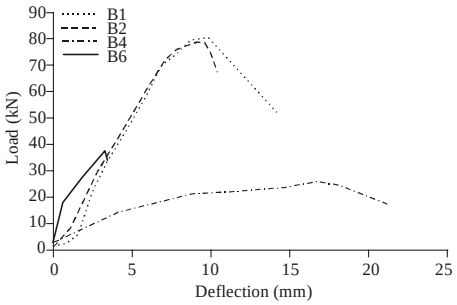

Fig. 11: Load deflection relationship of un-strengthened and strengthened beams with large square openings at distance d

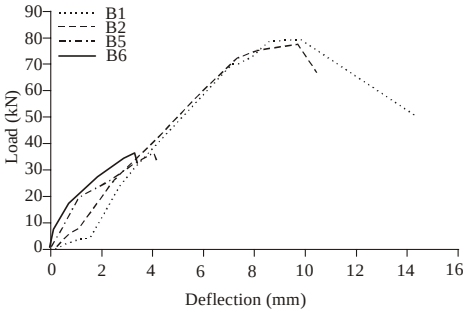

Fig. 12: Load deflection relationship of strengthened beams with large square openings at distance 0.5d and d

crushing of concrete at the bottom chord and support while peeling of CFRP laminates together with concrete cover was observed at the top chord.

Fig. 8b illustrates the RC beam with large square openings at distance d away from the support, beam B6. Similar to the mode of failure as observed in beam B5, flexural cracks was clearly shown along the tension zone of the beam followed by a sudden shear failure. The square opening near the right support was tilted upwards due to yielding of top and bottom steel reinforcement causing crushing of concrete at the top and bottom chord. Peeling of CFRP laminates was observed at the top and bottom chord above and below the opening, respectively. Due to the presence of CFRP laminates around the square openings, the initial crack at the four corners of the square openings was diverted into flexural cracks formed along the mid-span of the beam. The existence of CFRP laminates disturbs the path of crack propagation which required a higher energy to divert the cracks into flexural cracks along the mid-span. Hence, a larger beam capacity was achieved compared to un-strengthened beams.

Load versus deflection relationship: Figure 9-12 depict the load versus mid-span deflection relationship of beams. The load deflection curves of the control beams are for

Table 2 : Test results

Specimens	Ultimate load, P_u(kN)	$\Delta P = P_u - P_{u0ave}$(kN)	$\Delta P/P_{u0ave}$(%)	Displacement at P_u(mm)	Failure type
B1	P_{u01}= 80.39	P_{u0ave} = 79.40	-	9.50	
B2	P_{u02}= 78.41		-	9.13	
B3	20.29	-59.11	-74	8.37	
B4	24.79	-54.61	-69	17.62	Shear
B5	36.54	-42.86	-54	4.08	
B6	36.88	-42.52	-54	3.27	

comparison purposes. Figure 9 illustrates the load deflection relationship of un-strengthened beams, B3 and B4 and both control beams. From the figure, at earlier stages, the load deflection curves are closed to each other. When the load is increased, the changes in stiffness in both un-strengthened beams were observed. The stiffness of the beams was gradually reduced compared to both control beams. After the yielding of steel reinforcement, the load of both un-strengthened beams, B3 and B4 was gradually decreased. It was observed that beam B3 exhibited an early cracking-yielding-failure process compared to beam B4 which demonstrated a gradual increase in load before failure. A larger ductility was observed in beam B4.

Figure 10-11 show the load-deflection relationship of un-strengthened beams, B3 and B4 with their respective strengthened beams, B5 and B6. At earlier stages, the load-deflection curves of the strengthened beams by CFRP exhibited a larger stiffness compared to their respective un-strengthened beams. A slight decrease in stiffness was observed after the cracking stage. Following to the yielding of reinforcing bars, the strength and stiffness of the strengthened specimens were larger compared to the un-strengthened beams. After beam failure, the load deflection curve of the strengthened beams dropped and the trend almost correspond to those of the control beams.

Figure 12 compares the load deflection relationship of both strengthened beams with large square openings in shear region, B5 and B6. At the initial stage, the stiffness of both strengthened beams with CFRP was larger than the control beams. Similar load deflection curve trend was observed between beam B5 and B6 except that beam B6 exhibited slightly larger in stiffness.

Ultimate load and displacement: The displacement and ultimate strength , P_u of the specimens are given in Table 2. In the table, the changes in ultimate load between the load obtained for each specimens and the average ultimate load of both control beams are provided. Also, the ratio of ΔP to the average strength of the control specimens, $\Delta P/P_{u0ave}$ in percentage of each specimen is shown. The presence of large square openings in the shear region at distance 0.5d and d away from the support in the RC beams, B3 and B4 respectively causes a substantial decrease in beam capacity, approximately 74 and 69%, respectively. Obviously, the openings created at a distance 0.5d is much more critical compared to a distance d. When the RC beams with square openings were strengthened by CFRP laminates, beam B5 and B6, the CFRP laminates in the strengthening configuration managed to re-gain the beam strength to approximately 54% of the original beam structural capacity in both beams. In addition, the displacement at P_u of each beam specimens is listed in the table. It is obvious that the displacement of the specimens strengthened by CFRP laminates managed to reduce the deflection significantly compared to the deflection of un-strengthened and control beams.

Numerical results:

Load deflection relationship: The load deflection relationship of control beams, un-strengthened and strengthened beams with large square openings in shear region obtained from the finite element analysis are validated against the experimental results and illustrated in Fig. 13.

Figures 13a depicts the load deflection curves of control beams, B1 and B2 from experiments and FEM analysis. The control beams were solid beams without any openings. Similar trend of load deflection curves was observed between FEM and experimental results for the control beam. The FEM analysis predicts the beam to be stiffer and stronger. The possible cause for the difference in stiffness between the control beam in the experiment and the finite element analysis is due to the assumed perfect bond between concrete and steel reinforcement.

For the un-strengthened beams with large square openings in shear region at distance 0.5d and d away from the support, B3 and B4 which are shown in Fig. 13b, the results of both FEM models are close to each other, both demonstrated a stiffer trend than the experimental results. After the cracks started to appear, the perfect bond models increasingly overestimate the stiffness of the beam. Similar as in the control beams, the possible reason may be due to the assumed perfect bond condition between concrete and steel reinforcement.

The load deflection curves of the strengthened beams with CFRP fully wrapped around the large square openings in shear region at distance 0.5d and d away from the support, B5 and B6 are illustrated in Fig. 13c. After incorporating the bond slip model which defined in the discrete reinforcement properties of CFRP, almost

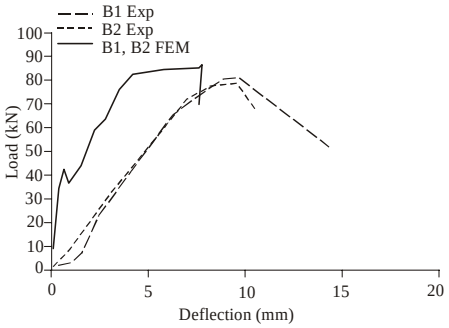

(a) Control beams

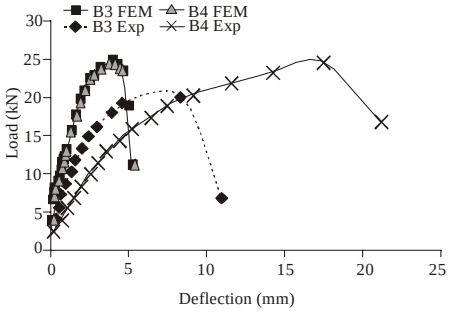

(b) Un Strengthened beams

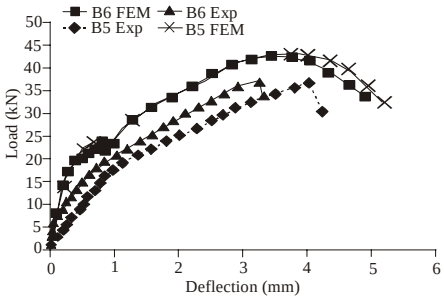

(c) Strengthened beams

Fig. 13: Load deflection relationship of beams, obtained by experiment and finite element method

similar trend was obtained between both FEM models compared to their respective experimental results. At early stage before initial crack, it was observed that the stiffness of beam B6 in finite element model are closely matching to the stiffness of experimental beam. Likewise, the second point of cracking at 1 mm deflection, a slight drop was observed in all FEM and experimental curves. In the range of yielding of reinforcement to failure, the load deflection curves of both FEM models were comparable with the load deflection curves of both experimental results.

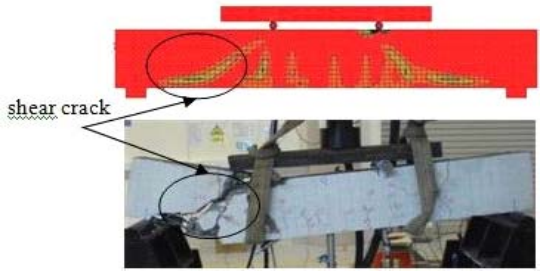

(a) Control beam

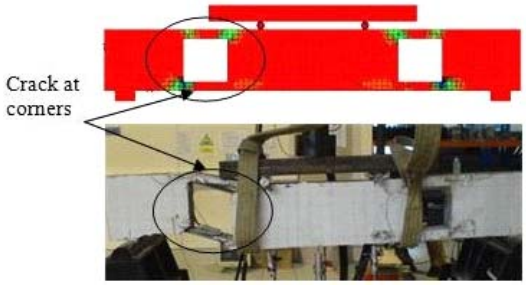

(b) B4

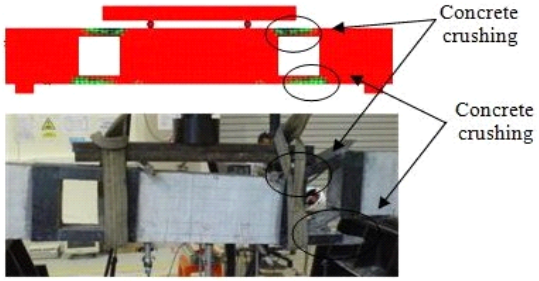

(c) B6

Fig. 14: Comparison between principal strain from FEM analysis and crack pattern from experiments

Crack pattern: Figure 14a-c illustrate a comparison between principal strain obtained from the finite element analysis and crack pattern obtained from the experiments of the control beam B1; un-strengthened beam with large square openings in shear region at distance d from the support, B4 and strengthened beam with CFRP fully wrapped around the large square openings in shear region at distance d from the support, B6. The cracks obtained in the experiments and in the simulations are observed similar. This indicates that the model can predict the mechanisms of fracture in the beams.

CONCLUSION

This investigation included the experimental testing of six reinforced concrete beams which comprised of control beams, un-strengthened and strengthened beams

with large square openings in shear region by CFRP laminates at a distance 0.5d and d away from the support. The strengthening configuration of CFRP laminates was a full wrapping system around the square openings. In addition, a two dimensional nonlinear finite element analysis was conducted to validate the results of the tested beams. Based on the findings of this study, the following conclusions can be made.

- In the early stage of un-strengthened beams, diagonal cracks were formed at the four corners of square openings and eventually leads to yielding of steel reinforcement and crushing of concrete cover. A brittle shear failure was observed.
- In the reinforced concrete beams, the presence of large square openings in shear region at distance 0.5d and d away from the support, B3 and B4 respectively causes a significant decrease in the beam capacity, approximately 74 and 69%, respectively. It was found that the losses of beam capacity due to the location of openings in shear, at distance 0.5d and d away from the support were almost similar.
- The CFRP laminates in the strengthening configuration managed to re-gain the beam strength of the RC beam with large square openings in shear region at distance 0.5d and d, B5 and B6, respectively to approximately 54% of the original structural capacity of beams.
- The predicted crack pattern in FEM shows good agreement with the crack pattern of the experimental beams. Meanwhile, the load mid-span deflection curves of the finite element models exhibited a stiffer result compared to the experimental beams. The possible reason may be due to the perfect bond assumption between the concrete and steel reinforcement.

ACKNOWLEDGMENT

The authors would like to extend their acknowledgments to the department of Civil Engineering, Universiti Teknologi PETRONAS for the excellent laboratory facilities and analytical tools and most importantly the continuous support for this research. Last but not least, the authors would like to acknowledge the lab technologists from Concrete Laboratory, department of Civil Engineering for their assistance during the experimental program.

REFERENCES

Abdalla, H.A., A. M. Torkey, H.A., Haggag and A.F. Abu-Amira, 2003. Design against cracking at openings in reinforced concrete beams strengthened with composite sheets. J. Compos. Struct., 60(2): 197-204.

Allam, S.M., 2005. Strengthening of rc beams with large openings in the shear zone. J. Eng. Alexandria, 44(1): 59-78.

Cervenka, V., L. Jendele and J. Cervenka, 2010. ATENA Program Documentation Part 1- Theory. Cervenka Consulting Ltd., Prague.

El Maaddawy, T. and S. Sherif, 2009. FRP composites for shear strengthening of reinforced concrete deep beams with openings. J. Compos. Struct., 89(1): 60-69.

Godat, A., P. Labossiere and K.W. Neale., 2011. Numerical investigation of the parameters influencing the behaviour of FRP shear-strengthened beams. Constr. Build. Mat., In Press http://dx. doi.org/10. 1016/j. conbuildmat. 2010.11.110

Godat, A., K.W Neale, P. Labossiere, 2007b. Towards modelling FRP shear-strengthened reinforced concrete beams. Proceedings of the 8th International Symposium on Fiber Reinforced Polymer Reinforcement for Concrete Structures, (FRPRCS' 2007), University of Patras, Patras, pp: 1-10

Kotynia, R., H.A. Baky, K.W. Neale, M. Asce and U.A. Ebead, 2008. Flexural strengthening of rc beams with externally bonded CFRP systems: Test results and 3D nonlinear FE analysis. J. Compos. Constr., 12(2): 190-201.

Lu, X.Z., J.G. Teng, L.P. Ye and J.J. Jiang, 2005. Bond-slip models for FRP sheets /plates bonded to concrete. Eng. Struct., 27(6): 920-937.

Madkour, H., 2009. Nonlinear analysis of strengthened rcbeams with web openings. Proceed. ICE-Struct. Build., 162(2):115-128.

Mansur, M.A., 2006. Design of reinforced concrete beams with web openings. Proceedings of the 6th Asia Pacific Structural Engineering and Construction Conference Kuala Lumpur, Sep. 5-6, pp:104-120.

Mansur, M.A. and K.H. Tan, 1999. Concrete Beams with Openings: Analysis and Design. CRC Press, New York, pp: 1-3

Mansur, M.A., K.H. Tan and W. Wei, 1999. Effects of creating an opening in existing beams. ACI Struct. J., 96(6): 899-906.

Mansur, M.A., L.M. Huang, K.H. Tan and S.L. Lee, 1992. Deflections of reinforced concrete beams with web openings. ACI Struct. J., 89(4): 391-397.

Obaidat, Y.T., S. Heyden and O. Dahlblom, 2010. The effect of CFRP and CFRP/concrete interface models when modelling retrofitted RC beams with FEM, J. Compos. Struct., 92(6): 1391-1398.

Pimanmas, A., 2010. Strengthening R/C beams with opening by externally installed FRP rods: Behaviour and analysis. J. Compos. Struct., 92(8): 1957-1976.